ERJ Express. Published on September 30, 2010 as doi: 10.1183/09031936.00015710

Malignant pleural effusion cells show aberrant glucose metabolism gene expression

Chien-Chung Lin[1,2], Lien-Chin Chen[3], Vincent S. Tseng[3], Jing-Jou Yan[4], Wu-Wei Lai[5], Wen-Pin Su[1,2], Chi-Hung Lin[6], Chi-Ying F. Huang[7], and Wu-Chou Su[1,2]

Correspondence to:

Wu-Chou Su
Division of Hematology/Oncology
Department of Internal Medicine
Hospital and College of medicine,
National Cheng Kung University College
138 Sheng-Li Road, Tainan 704, Taiwan
Tel: 886-6-235-3535 ext. 5401
Fax: 886-6-276-6175
E-mail: sunnysu@mail.ncku.edu.tw
and
Professor Chi-Ying F. Huang
Institute of Clinical Medicine
National Yang-Ming University
201, Sec. 2, Shih-Pai Road,
Peitou Taipei 11217, Taiwan
Tel: 886-2-2826-7000 ext. 7904
Fax: 886-2-2874-5074
E-mail: cyhuang5@ym.edu.tw

[1]Graduate Institute of Clinical Medicine, College of Medicine, and [3]Department of Computer Science and Information Engineering, College of Engineering, National Cheng Kung University
Departments of [2]Internal Medicine, [4]Pathology, and [5]Surgery, Hospital and College of medicine, National Cheng Kung University, Tainan, Taiwan
[6]Institute of Microbiology and Immunology and the [7]Institute of Clinical Medicine, National Yang-Ming University, Taipei, Taiwan

Journal category: Thoracic Oncology

Brief statement:

1. This study reports aberrantly regulated genes in lung adenocarcinoma cells from malignant pleural effusion.
2. The study highlights the importance of the glucose metabolic reprogramming in the pathogenesis of malignant pleural effusion.

ABSTRACT

Background: Malignant pleural effusion (MPE) accompanying lung adenocarcinoma indicates poor prognosis and early metastasis. This study aimed to identify genes related to MPE formation.

Methods: Three tissue sample cohorts - seven from healthy lungs, 18 from stage I-III lung adenocarcinoma with adjacent healthy lung tissue, and 13 from lung adenocarcinomas with MPE were analyzed by oligonucleotide microarray. The identified genes were verified by quantitative real-time polymerase chain reaction (qRT-PCR), immunohistochemical staining, and immunofluorescence confocal microscopy.

Results: Twenty up- or down-regulated genes with a two-fold change in MPE cancer cells compared to healthy tissues were differentially expressed from early- to late-stage lung cancer. Of 13 genes related to cellular metabolism, aldolase A (ALDOA), sorbitol dehydrogenase (SORD), transketolase (TKT), and tuberous sclerosis 1 (TSC1) were related to glucose metabolism. QRT-PCR validated their mRNA expressions in pleural metastatic samples. Immunohistochemical staining confirmed aberrant TKT, ALDOA, and TSC1 expressions in tumor cells. Immunofluorescence confirmed TKT co-localization and co-distribution of ALDOA with thyroid transcription factor 1 (TTF-1) positive cancer cells. TKT regulated the proliferation, vascular endothelial growth factor (VEGF) secretion *in vitro* and *in vivo* vascular permeability of cancer cell.

Conclusion: Glucose metabolic reprogramming by ALDOA, SORD, TKT, and TSC1 is important in MPE pathogenesis.

Key words: *Malignant pleural effusion, lung adenocarcinoma, glucose metabolism genes*

Abbreviations: MPE, malignant pleural effusion; ALDOA, aldolase A; SORD, sorbitol dehydrogenase; TKT, transketolase; TSC1, tuberous sclerosis, VEGF, vascular endothelial growth factor.

INTRODUCTION

Lung cancer is the leading cause of cancer death in both men and women in the United States, Europe, and Taiwan [1]. Its incidence is increasing and women are more likely than men to have an adenocarcinoma subtype [2], which is often complicated by malignant pleural effusion [3]. A recent study reports that majority of their 136 patients with lung adenocarcinoma and MPE were female (61%) [4]. Patients with MPE have been previously classified as stage IIIB but recent data from the International Association for the Study of Lung Cancer (IASLC) propose that the staging of lung cancers with concomitant MPE should be reclassified as early metastasis (M1a) [5].

Unlike other solid cancers with surrounding vascular structures to provide conduits for travel and nutrient delivery, cancer cells in MPE proliferate autonomously and have a high metastatic potential. Due to their specific biological properties, malignant cells within MPE are uniquely capable of surviving and proliferating without a solid-phase scaffolding [6]. Another important mediator is the vascular endothelial growth factor (VEGF), which contributes to the formation of malignant effusions by increasing vascular permeability [7]. Some genes in MPE may be so specific in maintaining the survival of cancer cells in MPE and VEGF secretions that MPE remains intractable and resistant to chemotherapy [8]. A previous study reveals that the IL6-Stat3-VEGF pathway [9] plays a key role in MPE formation. A connection between EGFR gene mutation and MPE has also been reported [4] but the specific genes or pathways dysregulated remain unexplored.

This study aimed to identify specific genes or pathways of adenocarcinoma with malignant pleural effusion and investigate their significance in MPE cancer cell survival and formation. It focused on female lung adenocarcinoma patients with MPE.

MATERIALS AND METHODS

MPE cancer cells, healthy normal lung tissue, and stage I-III lung cancer for microarray analysis

First, to identify differently expressed genes between MPE cancer cell and normal lung tissue, two cohorts for microarray analysis were collected. The institutional review board approved the study and all patients provided written informed consent. The first cohort of MPE was obtained from 13 women who underwent thoracentesis or thoracotomy at the National Cheng Kung Hospital (Tainan, Taiwan) from 2002 to 2005. Cytologic analysis or pathologic proof from pleural biopsy was used to verify each lung adenocarcinoma-associated MPE specimen. The methods used to collect cancer cells from MPE [10], RNA extraction, Affymetrix array hybridization, and image processing were shown in the annexed supplementary material and method. A second cohort of healthy lung tissue microarray was provided by Dr Chi-Hung Lin (National Yang-Ming University).

Secondly, the study aimed to show that MPE-specific genes were not only different from health lung tissue but also relatively up- or down-regulated compared to the primary tumor. The identified genes were MPE-specific and more metastatic and invasive than the primary tumor. However, the primary pulmonary tumor of MPE was often not available and no pairing analyses (primary tumor and MPE) could be done. Thus, a third cohort micro-array database set (NCBI Gene Expression Omnibus [GEO accession number: GSE7670]) [11], which included samples from 18 women with lung adenocarcinoma with adjacent healthy tissue. The basic and clinical characteristics of these three cohorts were listed in Table 1.

Statistical analysis of micro-array data

Using the Golub criteria [12] to identify differentially expressed genes between MPE and healthy normal lung tissue, the top 500 differential genes corresponding to 631 microarray probes were identified. These 500 discriminative genes (MPE-specific genes) were further analyzed using the third cohort microarray database set. The first and the third cohorts were pooled and classified as a fourth group including 18 adjacent normal lung tissue, 9 stage I lung cancer, 9 stage III, and 13 MPE cancer cell representing normal tissue to early stage lung cancer to late-stage (or pre-metastatic) stage.

After using Robust Multi-array analysis normalization [11], the 631 probes were further restricted by adding the criterion that the genes show a tendency to be expressed at higher or lower levels between the adjacent healthy, stage I, stage III, and MPE samples. First, the identified genes had to be differentially expressed between the four groups. One-way ANOVA was used to search for genes that were expressed statistically different among these four groups ($p<0.05$). Moreover, the expressions of these genes had to be higher in MPE compared to the tumor part of stage III cancer, higher in the tumor part of stage III cancer compared to that of stage I cancer, and higher in the tumor part of stage I cancer than the adjacent normal lung tissue. Otherwise, the expression of these genes had to be lower in MPE compared to the tumor part of stage III cancer, lower in the tumor part of stage III cancer compared to that of stage I cancer, and lower in the tumor part of stage I cancer than the adjacent normal lung tissue.

The identified up- or down-regulated genes in MPE cancer cells were also expressed differentially as the cancer progressed from early stage to MPE. Using these supervised and strict set of criteria among the four groups, 71 genes were identified from 500 genes. These 71 genes were further restricted to the expressions level at least two-fold higher in MPE samples than normal lung tissue, with $p<0.001$ to exclude false significant results [13]. The workflow for the analysis was shown in figure 1a.

RNA extraction and quantitative RT-PCR

RNA extraction and quantitative RT-PCR were done by Welgene Biotech Co., Ltd. (Taipei, Taiwan), while total RNA purification was done by TRIzol reagent combined spin columns. All samples were PCR-amplified (LightCycler-FastStart DNA Master SYBR Green I kit; Roche Diagnostics Corporation, Roche Applied Science, Indianapolis, IN, USA) with constitutively expressed β-actin. The primers designed for the identified genes were listed in Table 2.

Immunohistochemistry and immunofluorescent images

Immunohistochemistry and immunofluorescence analysis validated the gene expression in clinical specimens. The basic and clinical characteristics of the three validation cohorts were listed in Table 4. The MPE cell blocks were produced using the AgarCyto cell block method [14]. The methods and the antibodies used for immunohistochemistry and immunofluorescence were shown in the annexed supplementary material and method.

Cell lines, cell lysates, and Western blot

The PC14PE6/AS2 (AS2) cell line was from ascites generated from intra-peritoneal (i.p.) injection with PC14PE6 in the metastatic animal model [9]. The normal bronchial cell line (NL-20), lung adenocarcinoma cell line-A549, and H1650 were purchased from American Type Culture Collection (Rockville, MD, USA). The CL1-0 clonal cell line was provided by Dr. Pan-Chyr Yang.

Total protein from healthy lung lysates and cancer cell lines were extracted, blotted, and detected using antibodies against human TKT, ALDOA (Proteintech), TSC1 (Cell Signaling Technology, Inc., Beverly, MA, USA), and glyceraldehyde-3-phosphate dehydrogenase (GAPDH) (Santa Cruz Biotechnology, Inc, Santa Cruz, CA, USA).

Antibody binding was detected by electro-chemiluminescence (Amersham) based on the manufacturer's instructions.

TKT inhibitor and MTT test

Oxythiamine was purchased from Sigma Chemical Co. (St. Louis, MO, USA). A 3-(4,5-Dimethylthiazol-2-yl)-2,5-diphenyltetrazolium bromide (MTT) test was used to evaluate the anti-proliferation effect of oxythiamine.

Transfection with small interfering RNA (siRNA), proliferation analysis, colony formation assay, in vitro VEGF secretion and in vivo vascular permeability assay (Miles permeability assay)

Oligonucleotides representing siRNA against human TKT expression (TKT siRNA) and mismatch control oligonucleotides (scramble siRNA) were used (Invitrogen-Life Technologies, Carlsbad, CA, USA). The siRNA sequence that targeted TKT was 5′-AAAGAGGACAGCCAUGAUCUCUGCG-3′, while the scramble siRNA was the negative control. The PC14PE6/AS2 cells were transfected with siRNA for a final concentration of 50-100 nM by MicroPorator MP-100 (NanoEnTek, Seoul, South Korea).

The cell proliferation of PC14PE6/AS2 after transfection was detected by flow cytometry analysis with proliferation-associated antigen Ki-67 and cell colony formation assay (See Supplementary Method).

Transfected PC14PE6/AS2 cells were maintained in 60 mm ultra-low attachment plate (50000 cells per plate, Corning, Lowell, MA, USA) for 48 h to evaluate cell morphology, VEGF secretion *in vitro* and *in vivo* permeability assay (Miles permeability assay) [9] (See Supplementary Method).

Statistical analysis

Data were analyzed using Prism 4 (GraphPad Software, Inc., La Jolla, CA, USA). Differential expressions of specific genes between different stages were assessed by one-way analysis of variance (ANOVA) and by Bonferroni post hoc multiple comparisons. The area grade of immunohistochemistry between tumor and healthy samples was determined by the Mann-Whitney U test. Student's t test was used to determine differences between TKT siRNA and scramble-transfected PC14PE6/AS2 cells. Statistical significance was set at $p<0.05$.

RESULTS

Glucose metabolism regulatory genes were aberrantly regulated in MPE cancer cells

Twenty differentially expressed genes were identified between MPE and healthy adjacent lung tissue. Fourteen genes were up-regulated and six were down-regulated in MPE group compared to the healthy controls (fig. 1b). Their fold changes and annotation were list in Table 1. Functional annotation and pathway interaction of these genes was done using the BABELOMICS platform [15] and Ingenuity Pathways Analysis (IPA) [16]. Gene Ontology annotation of three of the 20 genes remained unestablished.

Combining IPA canonical pathway analysis and functional definitions with Gene Ontology and KEGG pathway analysis in the BABELOMICS platform, 13 of the 17 well-known genes (76%) were related to metabolic processes. Further studies of the 13 genes showed that three - aldolase A (ALDOA), sorbitol dehydrogenase (SORD), and transketolase (TKT) - were directly related to glucose metabolism (figs. 2a, 2b). Of the down-regulated genes, tuberous sclerosis 1 (TSC1) was involved in the insulin pathways, according to the KEGG database.

Whether these genes are differential expressed from healthy to early stage lung cancer to MPE were further investigated. The difference between stage I cancer and MPE was statistically significant (fig. 2c, $p<0.01$ in SORD and $p<0.05$ in ALDOA and TKT, all by Bonferroni multiple comparisons). The expression levels were also significantly different between the healthy and stage III samples in the three genes ($p<0.01$ in ALDOA, and $p<0.05$ in SORD and TKT). Expression levels of TSC1 were lower in the MPE samples than in the stage I ($p<0.01$) and III ($p<0.05$) samples.

To verify these gene expression data, RNA was extracted from nine metastatic pleurae lung adenocarcinoma and adjacent normal lung tissue. Samples were then analyzed using quantitative RT-PCR. ALDOA and TKT expressions were significantly

higher, while TSC1 and pantothenate kinase 2 (PANK2, a non-glucose-metabolism gene) expressions were significantly lower in tumor than in healthy samples (fig. 2d, $p<0.05$, by Student's *t*-test). SORD expression was also higher in tumor samples, but not statistically significant ($p=0.05$).

TKT and ALDOA protein expression was higher and TSC1 protein expression was lower in tumor cells than in healthy cells

Western blotting was used to test the protein expression levels of TKT, ALDOA, and TSC1 in four lung cancer cell lines: A549, PC14PE6/AS2, H1650, and CL 1-0. TKT and ALDOA expression were higher and TSC1 expression was lower in lung cancer cell lines than in healthy lung lysates (fig. 2e) and normal bronchial cell line (NL-20; supplementary fig.1). Immunohistochemical staining validated the protein expression in clinical samples of lung cancer tissue, adjacent healthy tissue, tumors invading the pericardium, and cancer cells from patients with MPE. TKT was located predominantly in the nucleus (figs. 3a, 3b) and was more abundantly expressed in tumor cells that invaded the pericardium (fig. 3c), and tumor tissue than in adjacent healthy bronchial epithelium.

Cancer cells from MPE were used to make AgarCyto cell blocks and to study TKT expression in MPE cancer cells. Cancer cells in MPE expressed high levels of TKT (fig. 3d). ALDOA expression, located predominately in cytoplasm, was higher in tumor cells than in adjacent healthy bronchial epithelial cells (figs. 3e, 3f). Tumor cells that invaded pericardium also expressed high ALDOA levels (fig. 3g). Conversely, TSC1, located primarily in the cytoplasm and nuclei, was expressed mainly in healthy pneumocytes but barely or not at all in tumor cells (figs. 3h, 3i).

Immunohistochemical analyses of 48 lung adenocarcinoma specimens showed that 19 were stage I, 13 stage II, 8 stage III, and 8 stage IV. The percentage of

immuno-reactive cancer cells was scaled using a four-tiered area grade and semi-quantitative system [17]. Using the area grade, the staining scores for TKT (fig. 3j, $p<0.001$) and ALDOA ($p<0.01$) were significantly higher in tumor tissue than in adjacent healthy tissue, and the staining score for TSC1 was significantly lower in tumor tissue ($p<0.001$) than in adjacent healthy tissue. A limited number of samples for each stage prevented further correlation studies of staining scores and cancer stages.

Cancer cell in MPE and pleural metastasis expressed high TKT and ALDOA

Thyroid transcription factor 1 (TTF-1) served as a good marker of lung cancer cells in MPE [18, 19]. To verify TKT and ALDOA expressions in lung cancer cells from MPE, eight MPE blocks from eight patients who underwent thoracocentesis and cancer cells were examined by cytology (Table 2). Triple immuno-staining using DAPI, TTF-1, TKT or ALDOA and recording under confocal microscope were used to investigate the expression and distribution of TKT and ALDOA in the TTF1 positive cells from MPE blocks. TTF-1 expression was predominant in the nucleus of cancer cells from MPE block while TKT immuno-reactivity was detected in the nuclei located within TTF1 positive cancer cells (fig. 4a).

The continuous section showed that ALDOA expression was detected in the cytoplasm and cell membrane within TTF1 positive cells (fig. 4b). Co-localization of TKT and co-expression of ALDOA in TTF1 positive cancer cell were also observed under lower power field with the acinar type (fig. 4c). Further quantitative analysis of ALDOA and TKT expression in the eight MPE cell blocks showed that the co-localization ratios of TKT and TTF1 were >70% (fig. 4d, using pixel-by-pixel analysis through by FV-1000 software) [20]. Defining co-expression of ALDOA as the distribution of ALDOA staining in more than one-third of the plasma membrane of TKT positive cells [20], the co-expression ratios were >75% (fig. 4d).

There were high TTF1, TKT and ALDOA expressions in metastatic pleural tissue by immunohistochemistry staining (fig. 5a). Immunofluorescence staining and photography by confocal microscope on the continuous section further confirmed the co-localization of TKT and co-expression of ALDOA in TTF1 positive cancer cells (fig. 5b). Immunohistochemical analyses of the metastatic pleural adenocarcinoma of ten patients (Table 4) showed that staining scores for TKT and ALDOA were significantly higher in tumor tissue compared to adjacent stroma and endothelial cell (fig. 5c and supplementary fig.2 ; $p<0.001$).

Oxythiamine and TKT knockdown with siRNA inhibited lung cancer cell proliferation

Oxythiamine, a well-known transketolase inhibitor, blocked TKT function by competing with thiamine, a key TKT co-factor [21]. It dose-dependently inhibited the proliferation of AS2, A549, CL1-0, and H1650 lung cancer cells 96 h after being added to the culture medium (fig. 6a). MTT assays showed that the IC_{50}s of all cells were around 10-20 mM.

To verify the role of transketolase on cancer cell proliferation, siRNA was used to knockdown TKT expression in PC14PE6/AS2 cells. The transfection of TKT siRNA into cells suppressed TKT expression but not in the scrambled and untransfected control, as assayed by Western blotting (fig. 6b). To investigate the effects of proliferation, the proportion of ki-67 staining (fig. 6c) was lower in TKT siRNA transfected cells (54%) than in the scramble control (74%). The rate of colony growth also decreased (20%) by colony formation assay (fig. 6d).

TKT knockdown with siRNA prevented lung cancer cell VEGF secretion in vitro and vascular permeability in vivo

Since cancer cells in the pleural cavity tended to be spheroid or clustered instead of flatten attachments in adherent culture dish, PC14PE6/AS2 cells were maintained in

ultra-low attachment plate to investigate the effects on knockdown TKT. Using TKT siRNA-to knockdown TKT expression, TKT siRNA cells dispersed instead of forming clusters (data not shown).

VEGF was a vascular permeability factor contributing the generation of malignant effusions [7]. First, ELISA of VEGF secretion of the conditioned medium revealed decreased VEGF secretions in si-TKT PC14PE6/AS2 cells compared to the si-scramble controls (fig. 7a).

The *in vivo* permeability assay (Miles permeability assay) was performed to understand if knockdown of TKT can down-regulate VEGF and lead to diminished vessel permeability. The areas of dye leakage induced by conditioned medium from TKT siRNA PC14PE6/AS2 cells were smaller than the leakage area from scramble transfected cells (figs. 7b, 7c). Thus, VEGF produced by PC14PE6/AS2 cells is biologically active, and that downregulation of VEGF secretion in PC14PE6/AS2 cells by inhibiting TKT can reduce vascular permeability.

DISCUSSION

Twenty genes are not only up-regulated (14) or down-regulated (6) in MPE cancer cell compared to normal lung tissue but also expressed differentially as lung cancer progresses from early stage to MPE. Of the 13 genes related to cell metabolism, three - ALDOA, SORD, and TKT - are directly involved in glucose metabolism while one, TSC1, is involved in the insulin pathway. Unlike other microarray studies derived directly from solid tumors, the MPE in this study has been collected from pleural metastatic lung adenocarcinoma and cancer cells have been further enriched as in a previous study [10]. Immunohistochemistry and immunofluorescence analysis of MPE

and metastatic pleural lesion further confirm the specificity of these genes in cancer cell other than in adjacent fibroblast and endothelium cell.

In 1924, Otto Warburg [22] proposed that tumor cells use glycolysis even in oxygen-rich environments and concluded that this defective metabolism results in cancer formation. Cancer cells in MPE proliferate autonomously and have a high metastatic potential [6]. Other investigators [23] have also demonstrated that low glucose concentrations and pH in the pleural effusion predicts shorter survival and less successful pleurodesis. An 18-F-2-deoxyglucose positron emission tomography (FDG-PET) study [24] shows that higher 18F-FDG uptake (higher glycolysis) in pleural effusion is associated with poor survival. Other glucose degradation pathways such as the pentose phosphate and sorbitol pathways have also been associated with cancer proliferation [25, 26].

Recently, many basic and clinical studies confirm that metabolic reprogramming benefits cancer cells [27]. Inhibiting glycolysis-associated enzymes blocks tumor growth in animal models. On the other hand, VEGF plays the key mediator in pleural effusion formation by increasing vascular permeability [7]. Many studies demonstrate the linkage between glycolysis and VEGF activation. Though hypoxia is a definite VEGF trigger [28], normoxic cells or cancer cell exposed to inflammatory stimuli like IFN, TNF-α, and interleukin may manifest phenotypic changes as those observed in hypoxic cells [29]. These inflammatory stimuli also induce VEGF secretion in lung cancer with MPE [9, 30]. The product of glycolysis-lactate has also been proven to incite angiogenesis even under normoxic environment [31].

In the current study, ALDOA, TKT, and SORD are all involved in glucose metabolism. There are three Aldolase isozymes in humans and ALDOA expression is higher in lung tumor than in healthy tissue [32]. The mechanism for this up-regulation

remains unknown. SORD is involved in the sorbitol pathway of glucose metabolism and although no studies have linked SORD to tumorigenesis, blocking the sorbitol pathway suppresses colon cancer cell proliferation [26]. TKT, the key enzyme in the pentose phosphate pathway, which mediates the conversion of glucose to ribose phosphate, is used in the biosynthesis of nucleic acids and nucleotides. The pentose phosphate pathway is up-regulated in cells with anchorage-independent cell growth phenotype [33], which have high metastatic potential. Cancer cells that proliferate in MPE are also anchorage independent.

TKT expression is not only higher in MPE in micro-array analysis but also verified in primary lung cancer tissue, metastatic pleural tumor, and malignant pleural effusion. Using the TKT inhibitor, oxythiamine, or transfecting lung cancer cell with small interfering RNA against TKT, inhibiting TKT suppresses lung cancer cell proliferation. Therefore, up-regulating TKT in cancer cells from MPE may facilitate their survival by activating the pentose phosphate pathway. Using an ultra-low attachment plate, the knockdown of TKT prevents cell aggregation, which is related to colony formation in soft agar [34]. TKT also controls the secretions of VEGF and vascular permeability *in vitro* and *in vivo*. A recent study in a diabetic animal model also verifies that the TKT activator (Benfotiamine) stimulates the activity of pentose phosphate pathway enzymes, leading to phosphorylation/activation of VEGF receptor-2 [35]. Taken together, TKT is involved not only in MPE cancer cell proliferation but also in VEGF secretion in MPE formation.

The TSC1/TSC2 complex is associated with the development of tuberous sclerosis, and mutations in either gene are responsible for both the familial and sporadic forms. Although not directly involved in glucose metabolism, TSC1 modulates the mTOR pathway and receives input from the PI3K-Akt and LKB1-AMPK pathways.

Hyper-activation of mTOR alone is sufficient to drive HIF-dependent transcription of glycolytic and angiogenesis-related genes [36]. The LKB1 gene is inactivated in lung cancer cells and related to tumorigenesis and metastasis [37]. Moreover, TSC1 regulates VEGF expression via the mTOR pathway [38]. Considering all of these, the AMPK-LKB1-TSC1 pathway is a potential target for lung cancer therapy.

In conclusion, a panel of genes from MPE may contribute to lung cancer progression. Glucose metabolism is important not only in tumorigenesis but also in cancer cell proliferation and VEGF secretion in MPE. This study increases the understanding of underlying mechanisms of MPE, which may facilitate the development of new treatment strategies for MPE-associated lung adenocarcinoma.

ACKNOWLEDGMENTS

This work was supported by the Department of Health (DOH99-TD-C-111-003, DOH99-TD-B-111-102), the NSC 97-2314-B-006-014-MY2, and by grants NHRI93A1-NSCBS04-2-5. The authors thank Dr. Fidler (MD Anderson Cancer Center, Houston, TX) for the human lung adenocarcinoma cell line PC14PE6, Dr. Pan-Chyr Yang (National Taiwan University College of Medicine, Taiwan) for the human lung adenocarcinoma cell line CL 1-0. The authors thank the Microarray & Gene Expression Analysis Core Facility of the National Yang-Ming University VGH Genome Research Center for the technical support and Dr. Eric Y. Chuang (Bioinformatics and Biostatistics Core, National Taiwan University) for the help with the Ingenuity Pathway Analysis. The authors also thank Dr. Gene Alzona Nisperos for the editing.

REFERENCES

1. Spiro SG, Silvestri GA. One hundred years of lung cancer. *American journal of respiratory and critical care medicine* 2005: 172(5): 523-529.

2. Coscio AM, Garst J. Lung cancer in women. *Current oncology reports* 2006: 8(4): 248-251.

3. Trompezinski S, Denis A, Schmitt D, Viac J. IL-10 is unable to downregulate VEGF expression in human activated keratinocytes. *Arch Dermatol Res* 2002: 294(8): 377-379.

4. Wu SG, Gow CH, Yu CJ, Chang YL, Yang CH, Hsu YC, Shih JY, Lee YC, Yang PC. Frequent EGFR mutations in malignant pleural effusion of lung adenocarcinoma. *Eur Respir J* 2008: 32(4):924-30.

5. Postmus PE, Brambilla E, Chansky K, Crowley J, Goldstraw P, Patz EF, Jr., Yokomise H. The IASLC Lung Cancer Staging Project: proposals for revision of the M descriptors in the forthcoming (seventh) edition of the TNM classification of lung cancer. *J Thorac Oncol* 2007: 2(8): 686-693.

6. Kassis J, Klominek J, Kohn EC. Tumor microenvironment: what can effusions teach us? *Diagnostic cytopathology* 2005: 33(5): 316-319.

7. Zebrowski BK, Yano S, Liu W, Shaheen RM, Hicklin DJ, Putnam JB, Jr., Ellis LM. Vascular endothelial growth factor levels and induction of permeability in malignant pleural effusions. *Clin Cancer Res* 1999: 5(11): 3364-3368.

8. Walker-Renard PB, Vaughan LM, Sahn SA. Chemical pleurodesis for malignant pleural effusions. *Annals of internal medicine* 1994: 120(1): 56-64.

9. Yeh HH, Lai WW, Chen HH, Liu HS, Su WC. Autocrine IL-6-induced Stat3 activation contributes to the pathogenesis of lung adenocarcinoma and malignant pleural effusion. *Oncogene* 2006: 25(31): 4300-4309.

10. Chen YM, Tsai CM, Whang-Peng J, Perng RP. Double signal stimulation was required for full recovery of the autologous tumor-killing effect of effusion-associated lymphocytes. *Chest* 2002: 122(4): 1421-1427.

11. Su LJ, Chang CW, Wu YC, Chen KC, Lin CJ, Liang SC, Lin CH, Whang-Peng J, Hsu SL, Chen CH, Huang CY. Selection of DDX5 as a novel internal control for

Q-RT-PCR from microarray data using a block bootstrap re-sampling scheme. *BMC genomics* 2007: 8: 140.

12. Golub TR, Slonim DK, Tamayo P, Huard C, Gaasenbeek M, Mesirov JP, Coller H, Loh ML, Downing JR, Caligiuri MA, Bloomfield CD, Lander ES. Molecular classification of cancer: class discovery and class prediction by gene expression monitoring. *Science (New York, NY* 1999: 286(5439): 531-537.

13. Landsittel D, Donohue-Babiak N. Effect of adding fold-change criteria to significance testing of microarray data. *Journal of Statistical Computation and Simulation* 2010: 80(1): 89 - 97.

14. Kerstens HM, Robben JC, Poddighe PJ, Melchers WJ, Boonstra H, de Wilde PC, Macville MV, Hanselaar AG. AgarCyto: a novel cell-processing method for multiple molecular diagnostic analyses of the uterine cervix. *J Histochem Cytochem* 2000: 48(5): 709-718.

15. Al-Shahrour F, Minguez P, Tarraga J, Montaner D, Alloza E, Vaquerizas JM, Conde L, Blaschke C, Vera J, Dopazo J. BABELOMICS: a systems biology perspective in the functional annotation of genome-scale experiments. *Nucleic acids research* 2006: 34(Web Server issue): W472-476.

16. Jimenez-Marin A, Collado-Romero M, Ramirez-Boo M, Arce C, Garrido JJ. Biological pathway analysis by ArrayUnlock and Ingenuity Pathway Analysis. *BMC proceedings* 2009: 3 Suppl 4: S6.

17. Barnes DM, Harris WH, Smith P, Millis RR, Rubens RD. Immunohistochemical determination of oestrogen receptor: comparison of different methods of assessment of staining and correlation with clinical outcome of breast cancer patients. *British journal of cancer* 1996: 74(9): 1445-1451.

18. Gomez-Fernandez C, Jorda M, Delgado PI, Ganjei-Azar P. Thyroid transcription factor 1: a marker for lung adenoarinoma in body cavity fluids. *Cancer* 2002: 96(5): 289-293.

19. Szczepulska-Wojcik E, Langfort R, Roszkowski-Sliz K. [A comparative evaluation of immunohistochemical markers for the differential diagnosis between malignant mesothelioma, non-small cell carcinoma involving the pleura, and benign reactive mesothelial cell proliferation]. *Pneumonol Alergol Pol* 2007: 75(1): 57-69.

20. Chen YF, Chou CY, Wilkins RJ, Ellory JC, Mount DB, Shen MR. Motor protein-dependent membrane trafficking of KCl cotransporter-4 is important for cancer cell invasion. *Cancer Res* 2009: 69(22): 8585-8593.

21. Rais B, Comin B, Puigjaner J, Brandes JL, Creppy E, Saboureau D, Ennamany R, Lee WN, Boros LG, Cascante M. Oxythiamine and dehydroepiandrosterone induce a G1 phase cycle arrest in Ehrlich's tumor cells through inhibition of the pentose cycle. *FEBS letters* 1999: 456(1): 113-118.

22. Warburg O. On the origin of cancer cells. *Science (New York, NY* 1956: 123(3191): 309-314.

23. Sanchez-Armengol A, Rodriguez-Panadero F. Survival and talc pleurodesis in metastatic pleural carcinoma, revisited. Report of 125 cases. *Chest* 1993: 104(5): 1482-1485.

24. Duysinx B, Corhay JL, Larock MP, Nguyen D, Bury T, Hustinx R, Louis R. Prognostic value of metabolic imaging in non-small cell lung cancers with neoplasic pleural effusion. *Nuclear medicine communications* 2008: 29(11): 982-986.

25. Langbein S, Zerilli M, Zur Hausen A, Staiger W, Rensch-Boschert K, Lukan N, Popa J, Ternullo MP, Steidler A, Weiss C, Grobholz R, Willeke F, Alken P, Stassi G, Schubert P, Coy JF. Expression of transketolase TKTL1 predicts colon and urothelial cancer patient survival: Warburg effect reinterpreted. *British journal of cancer* 2006: 94(4): 578-585.

26. Tammali R, Ramana KV, Srivastava SK. Aldose reductase regulates TNF-alpha-induced PGE2 production in human colon cancer cells. *Cancer letters* 2007: 252(2): 299-306.

27. Kroemer G, Pouyssegur J. Tumor cell metabolism: cancer's Achilles' heel. *Cancer cell* 2008: 13(6): 472-482.

28. Ryan HE, Lo J, Johnson RS. HIF-1 alpha is required for solid tumor formation and embryonic vascularization. *EMBO J* 1998: 17(11): 3005-3015.

29. Lutz NW, Tome ME, Cozzone PJ. Early changes in glucose and phospholipid metabolism following apoptosis induction by IFN-gamma/TNF-alpha in HT-29 cells. *FEBS letters* 2003: 544(1-3): 123-128.

30. Stathopoulos GT, Kollintza A, Moschos C, Psallidas I, Sherrill TP, Pitsinos EN, Vassiliou S, Karatza M, Papiris SA, Graf D, Orphanidou D, Light RW, Roussos C,

Blackwell TS, Kalomenidis I. Tumor necrosis factor-alpha promotes malignant pleural effusion. *Cancer Res* 2007: 67(20): 9825-9834.

31. Hunt TK, Aslam R, Hussain Z, Beckert S. Lactate, with oxygen, incites angiogenesis. *Adv Exp Med Biol* 2008: 614: 73-80.

32. Ojika T, Imaizumi M, Watanabe H, Abe T, Kato K. [An immunohistochemical study on three aldolase isozymes in human lung cancer]. *[Zasshi] [Journal]* 1992: 40(3): 382-386.

33. Mori S, Chang JT, Andrechek ER, Matsumura N, Baba T, Yao G, Kim JW, Gatza M, Murphy S, Nevins JR. Anchorage-independent cell growth signature identifies tumors with metastatic potential. *Oncogene* 2009: 28(31): 2796-2805.

34. Zhang X, Xu LH, Yu Q. Cell aggregation induces phosphorylation of PECAM-1 and Pyk2 and promotes tumor cell anchorage-independent growth. *Mol Cancer* 2010: 9: 7.

35. Katare R, Andrea C, Emanueli C, Madeddu P. Benfotiamine improves functional recovery of the infarcted heart via activation of pro-survival G6PD/Akt signaling pathway and modulation of neurohormonal response. *Journal of Molecular and Cellular Cardiology*: In Press, Uncorrected Proof.

36. Kwiatkowski DJ, Manning BD. Tuberous sclerosis: a GAP at the crossroads of multiple signaling pathways. *Human molecular genetics* 2005: 14 Spec No. 2: R251-258.

37. Ji H, Ramsey MR, Hayes DN, Fan C, McNamara K, Kozlowski P, Torrice C, Wu MC, Shimamura T, Perera SA, Liang MC, Cai D, Naumov GN, Bao L, Contreras CM, Li D, Chen L, Krishnamurthy J, Koivunen J, Chirieac LR, Padera RF, Bronson RT, Lindeman NI, Christiani DC, Lin X, Shapiro GI, Janne PA, Johnson BE, Meyerson M, Kwiatkowski DJ, Castrillon DH, Bardeesy N, Sharpless NE, Wong KK. LKB1 modulates lung cancer differentiation and metastasis. *Nature* 2007: 448(7155): 807-810.

38. Lee DF, Kuo HP, Chen CT, Hsu JM, Chou CK, Wei Y, Sun HL, Li LY, Ping B, Huang WC, He X, Hung JY, Lai CC, Ding Q, Su JL, Yang JY, Sahin AA, Hortobagyi GN, Tsai FJ, Tsai CH, Hung MC. IKK beta suppression of TSC1 links inflammation and tumor angiogenesis via the mTOR pathway. *Cell* 2007: 130(3): 440-455.

Table 1. Characteristic of three female cohorts for array analysis

Variable	Stage*	Age
Normal healthy women		58.0±8.7
18 Lung cancer	9 stage I (3 IA& 6 IB)	59.7±7.9
	9 stage III (5 IIIA & 4 IIIB)	
13 MPE	5 IIIB	57.5±10.8
	8 IV	

*stage according to American Joint Committee on Cancer (AJCC, 1997)

Table 2. List of differentially expressed genes between MPE and normal lung tissue*

Clone	Symbol	Description	Fold change
201563_at	SORD	sorbitol dehydrogenase	4.48
200776_s_at	BZW1	basic leucine zipper and W2 domains 1	4.11
208699_x_at	TKT	Transketolase	3.38
201577_at	NME1	non-metastatic cells 1, protein (NM23A)	3.29
219288_at	C3orf14	chromosome 3 open reading frame 14	3.25
200966_x_at	ALDOA	aldolase A,	3.14
218027_at	MRPL15	mitochondrial ribosomal protein L15	2.78
210058_at	MAPK13	mitogen-activated protein kinase 13	2.61
206052_s_at	SLBP	stem-loop (histone) binding protein	2.58
217835_x_at	C20orf24	chromosome 20 open reading frame 24	2.48
207543_s_at	P4HA1	procollagen-proline, 2-oxoglutarate 4-dioxygenase (proline 4-hydroxylase)	2.42
208828_at	POLE3	polymerase (DNA directed), epsilon 3 (p17 subunit)	2.31
201653_at	CNIH	cornichon homolog	2.19
203517_at	MTX2	metaxin 2	2.02
221016_s_at	TCF7L1	transcription factor 7-like 1	0.47
209390_at	TSC1	tuberous sclerosis 1	0.45
209002_s_at	CALCOCO1	calcium binding and coiled-coil domain 1	0.44
218552_at	ECHDC2	enoyl Coenzyme A hydratase domain containing 2	0.40
218809_at	PANK2	pantothenate kinase 2	0.36
215111_s_at	TSC22D1	TSC22 domain family, member 1	0.23

*fold change>2 or <0.5; $p<0.001$

Table 3. RT-PCR primers of selected genes for the Lightcycler

gene symbol	sense primer	antisense primer
TSC1	Tgggaattggaatcaaaagag	acaagcaactgccttgacatt
SORD	Tgaccaccgtacccctactg	cagacttggacgcaagcat
ALDOA	Ggcctccgtctggatttc	gggcatggtgctggtagtag
TKT	Atgccattgcacaagctg	cacacttcatacccgcccta
PANK2	Ggtcttggcaatcatctgtg	cccttccaaaaactgcttgt

Table 4. Characteristic of three cohorts for validation

Variable	Sex	Stage	Age
Immunohistochemistry of normal lung tissue and adjacent	28male 20female	11 stage IA, 8 stage IB, 7 stage IIA, 6 stage IIA 6 stage IIIA, 2 stage IIIB 8 stage IV	57.4±11.3
10 metastatic pleurae	6 female 4 male	4 stage IIIB 6 stage IV	56.9±15.8
8 MPE block	4 female 4 male	1 stage IIIB 7 stage IV	63±10.2

LEGEND

Figure 1. Flow chart for collecting three different cohorts for microarray analysis and gene expression profiles clustered hierarchically based on final 20 genes.

FIGURE 1.

a)

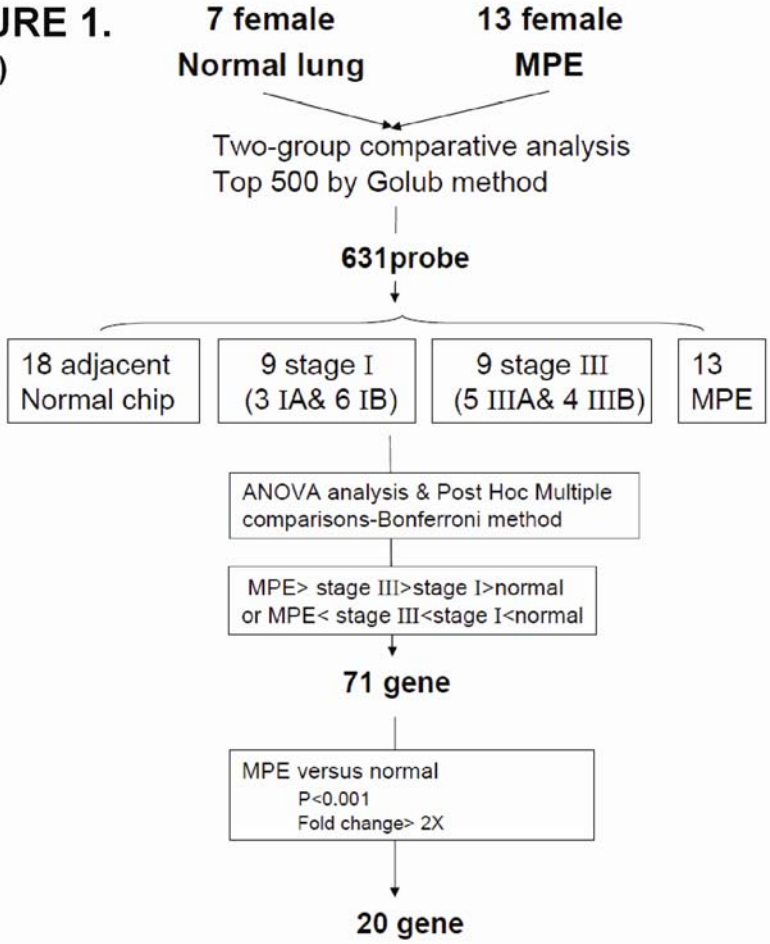
7 female
Normal lung
13 female
MPE
Two-group comparative analysis
Top 500 by Golub method
631probe
18 adjacent Normal chip
9 stage I (3 IA& 6 IB)
9 stage III (5 IIIA& 4 IIIB)
13 MPE
ANOVA analysis & Post Hoc Multiple comparisons-Bonferroni method
MPE> stage III>stage I>normal
or MPE< stage III<stage I<normal
71 gene
MPE versus normal
P<0.001
Fold change> 2X
20 gene

b)

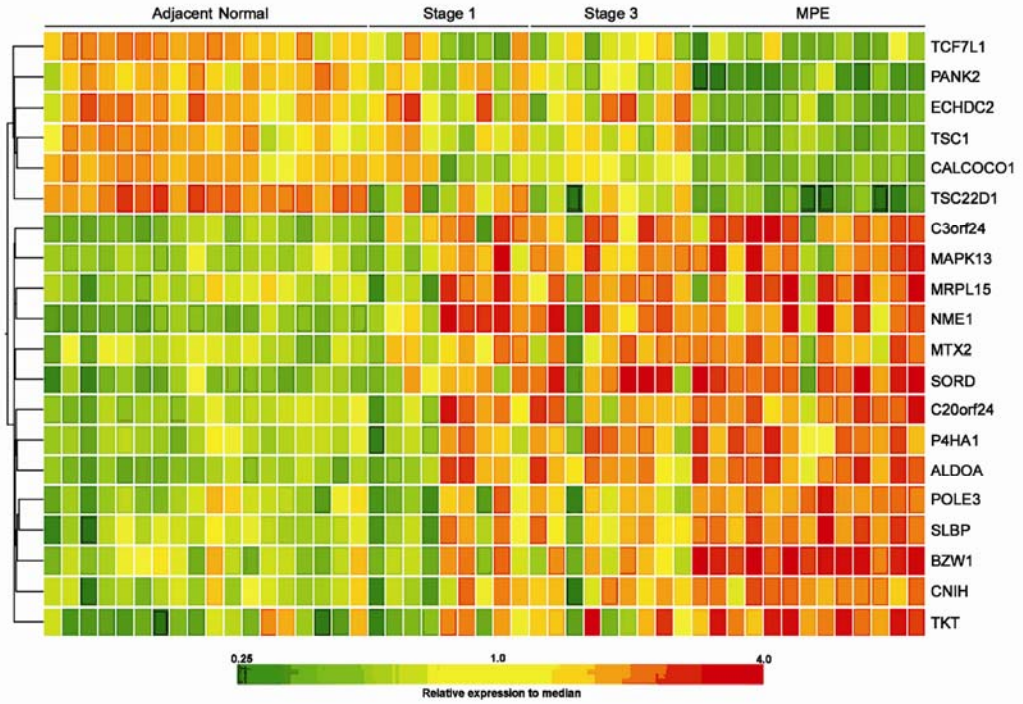
Adjacent Normal
Stage 1
Stage 3
MPE
TCF7L1
PANK2
ECHDC2
TSC1
CALCOCO1
TSC22D1
C3orf24
MAPK13
MRPL15
NME1
MTX2
SORD
C20orf24
P4HA1
ALDOA
POLE3
SLBP
BZW1
CNIH
TKT
0.25
1.0
4.0
Relative expression to median

Figure 2. Analyze all genes and selected gene expression in different stages of lung cancer toward bioinformatics platform, qRTPCR of tissue samples and Western blotting of lung cancer cell lines. (a) The BABELOMICS platform revealed that most genes were associated with cell metabolism, according to the Gene Ontology database. Y-axis, percentage of well-known genes associated with a specific biological function or pathway. (b) Ingenuity Pathways analysis of all genes was displayed by canonical pathway. Y-axis indicated the significance (–log *p* value, threshold = $p<0.05$) of the pathway association. (c) Gene expression values of glycolysis-associated genes (TSC1, SORD, ALDOA, TKT) from healthy controls and lung cancer patients at different stages (using Robust Multi-array Analysis normalization (*$p<0.05$; **$p<0.01$; ***$p<0.001$). (d) Quantitative real-time PCR analysis of TSC1, SORD, ALDOA, TKT, and PANK2 from four lung cancer and adjacent healthy lung tissue samples (*$p<0.05$). (e) Western blotting was used to detect TKT, ALDOA (PC14PE6/AS2, A549, H1650, CL1-0) and TSC1 (PC14PE6/AS2, A549, CL1-0) expressions in the lysates from healthy lung and lung cancer cell lines.

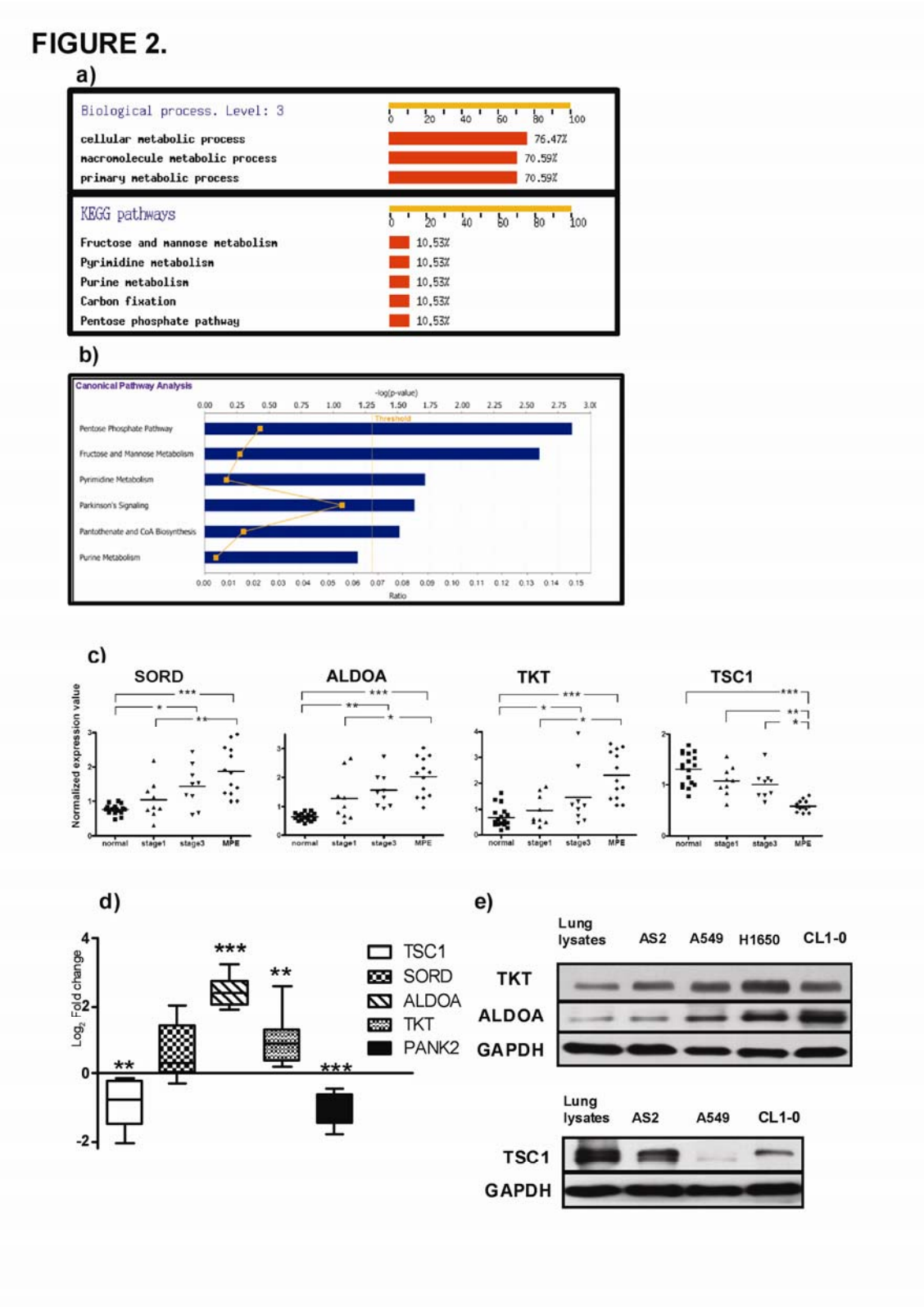

Figure 3. Immunohistochemical staining of TKT, ALDOA, and TSC1 in clinical specimens. (a) TKT intensity in healthy bronchiole epithelium (arrow, 20× objective). (b) Nucleus immuno-reactive TKT predominantly expressed in the lung

adenocarcinoma adjacent to healthy bronchiole epithelium (arrowhead, 20× objective). (c) TKT expression in lung cancer cells invading the pericardium (40× objective). (d) TKT intensity of cancer cells in malignant pleural effusion (40× objective). (e) Cytoplasmic localization of predominant ALDOA in lung adenocarcinoma (arrowhead, 20× objective) adjacent to the healthy bronchiole epithelium (arrow, 20× objective). (f) ALDOA intensity in lung adenocarcinoma. (g) ALDOA expression in lung cancer cells invading the pericardium (40× objective). (h) Nuclear and cytoplasmic expression of TSC1 in pneumocytes (arrow, 20× objective). (i) No expression of TSC1 in adjacent tumor tissue (20× objective).(j) Immunohistochemical analysis of TKT, ALDOA, and TSC1 expression in tumor and adjacent healthy tissue specimens from 48 patients (semi-quantitative area scores: 0, no stained tumor cells; 1, 0-25% of tumor cells stained; 2, 26-50% tumor cells stained; 3, 51-75% tumor cells stained; 4, 76-100% tumor cells stained. $^{**}p<0.01$; $^{***}p<0.001$). Higher TKT, higher ALDOA, and lower TSC1 expression in tumor tissue compared to the adjacent healthy area.

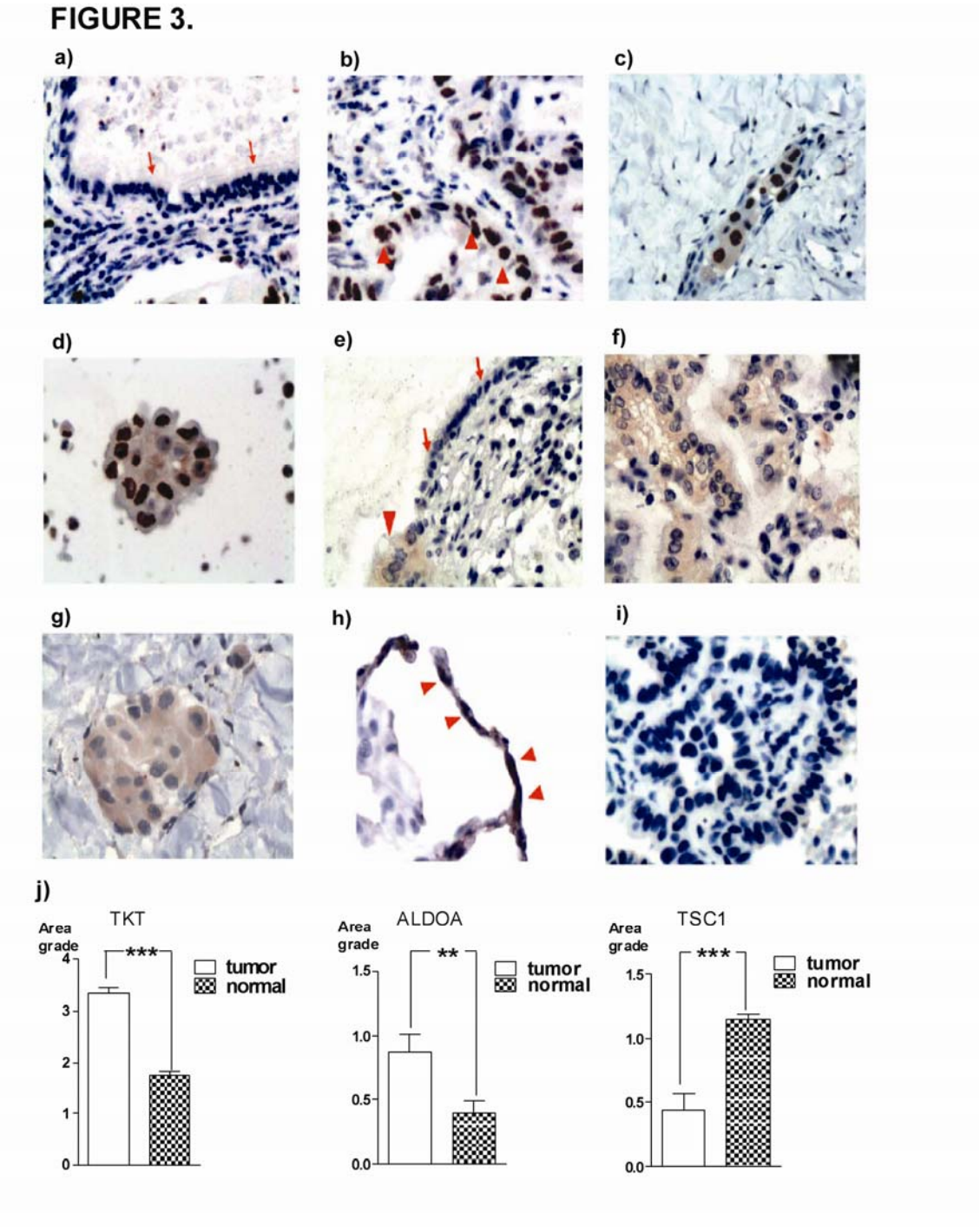

Figure 4. Immunofluorescent analysis detected the expression and distribution of TKT, ALDOA and TTF-1 at MPE lung cancer cells. (a) Confocal image under higher power field (60× objective) showed the immuno-detection of TTF-1 at nucleus

demonstrated by DAPI stain for nucleus, TTF-1 stain, merge of DAPI stain and TTF-1 stain and merge of TTF-1 and DIC (differential interference contrast) images. The co-localization of TTF-1 and TKT was verified by TKT stain and merge of TTF-1 and TKT stain. (b) Continuous section showed simultaneous immunodetection of TTF1 and ALDOA (cytoplasma and cell membrane) by DAPI stain, TTF1 stain, ALDOA stain and merge of TTF-1 and ALDOA stain. (c) Representative confocal images under low power field (20× objective) showed co-localization of TKT and TTF1 in nucleus and cytoplasm distribution of ALDOA in TTF-1(+) MPE cancer cells. (d) Immunofluorescent analysis was used to detect the co-localization ratio between TTF-1 and TKT (pixel-by-pixel analyses), and ratio of cytoplasm co-distribution of ALDOA in TTF-1(+) cancer cell from 8 patients' MPE cell blocks.

FIGURE 4.

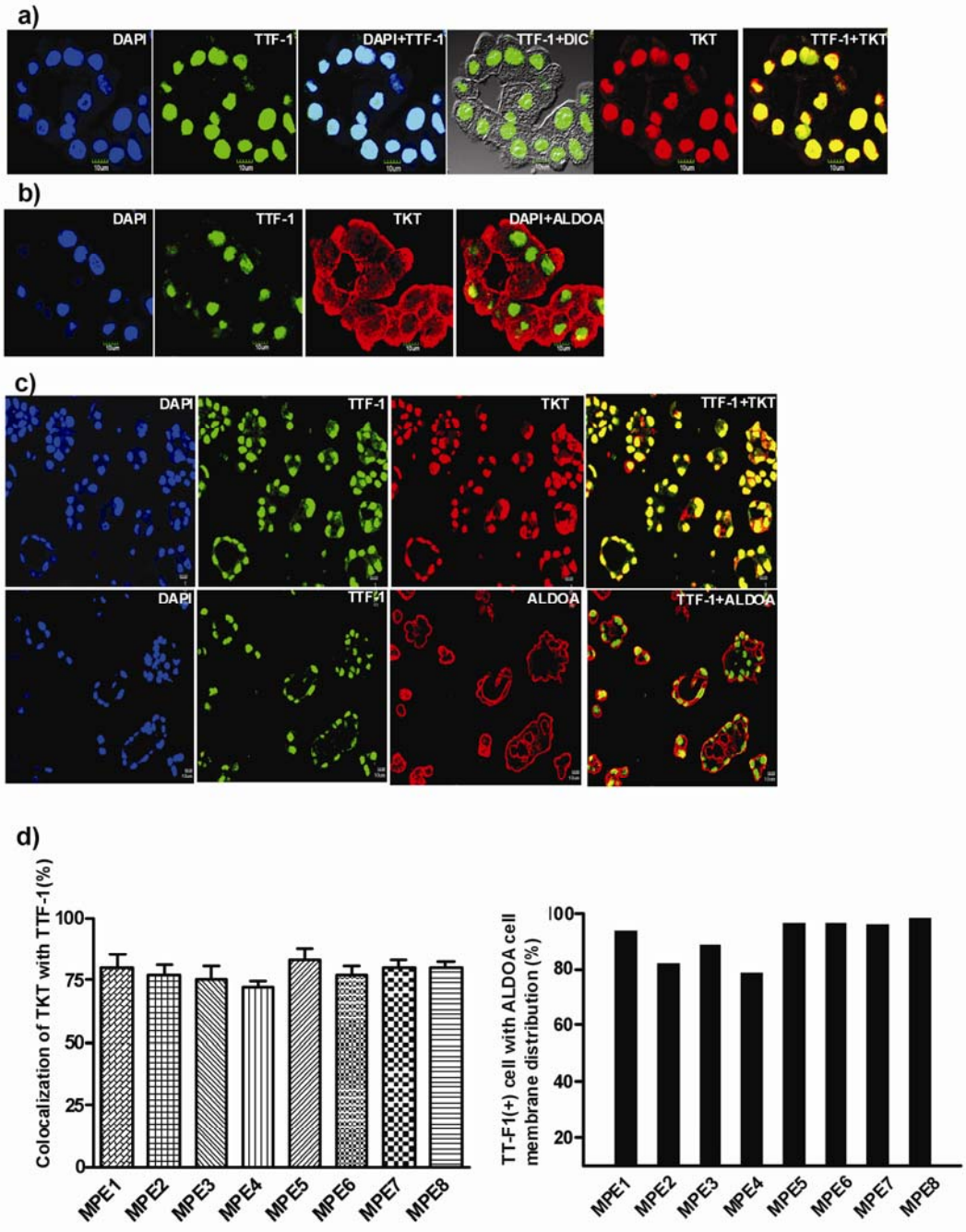

Figure 5. Distribution of TKT, ALDOA and TFT at metastatic pleurae tumor. (a) Immunohistochemical analysis was used to detect the expression of TKT, ALDOA, and TTF1 in metastatic pleurae tumor (area of dash line, 20× objective) compared to adjacent normal pleurae tissue. (b) Continuous section for immunofluorescence

analysis and confocal image showed co-localization of TKT and TTF-1 in nucleus and cytoplasmic distribution of ALDOA in TTF-1(+) cancer cell in metastatic pleurae tumor (area of dash line, 20× objective). (c) Immunohistochemical analysis was used to detect the expression of TKT and ALDOA of 10 patients' metastatic pleurae tumor. Higher expression of TKT and ALDOA in tumor tissue compared with the adjacent fibroblast and endothelial cell. (semi-quantitative area scores: 0, no stained tumor cells; 1, 0-25% of tumor cells stained; 2, 26-50% tumor cells stained; 3, 51-75% tumor cells stained; 4, 76-100% tumor cells stained. ***$p < 0.001$).

FIGURE 5.

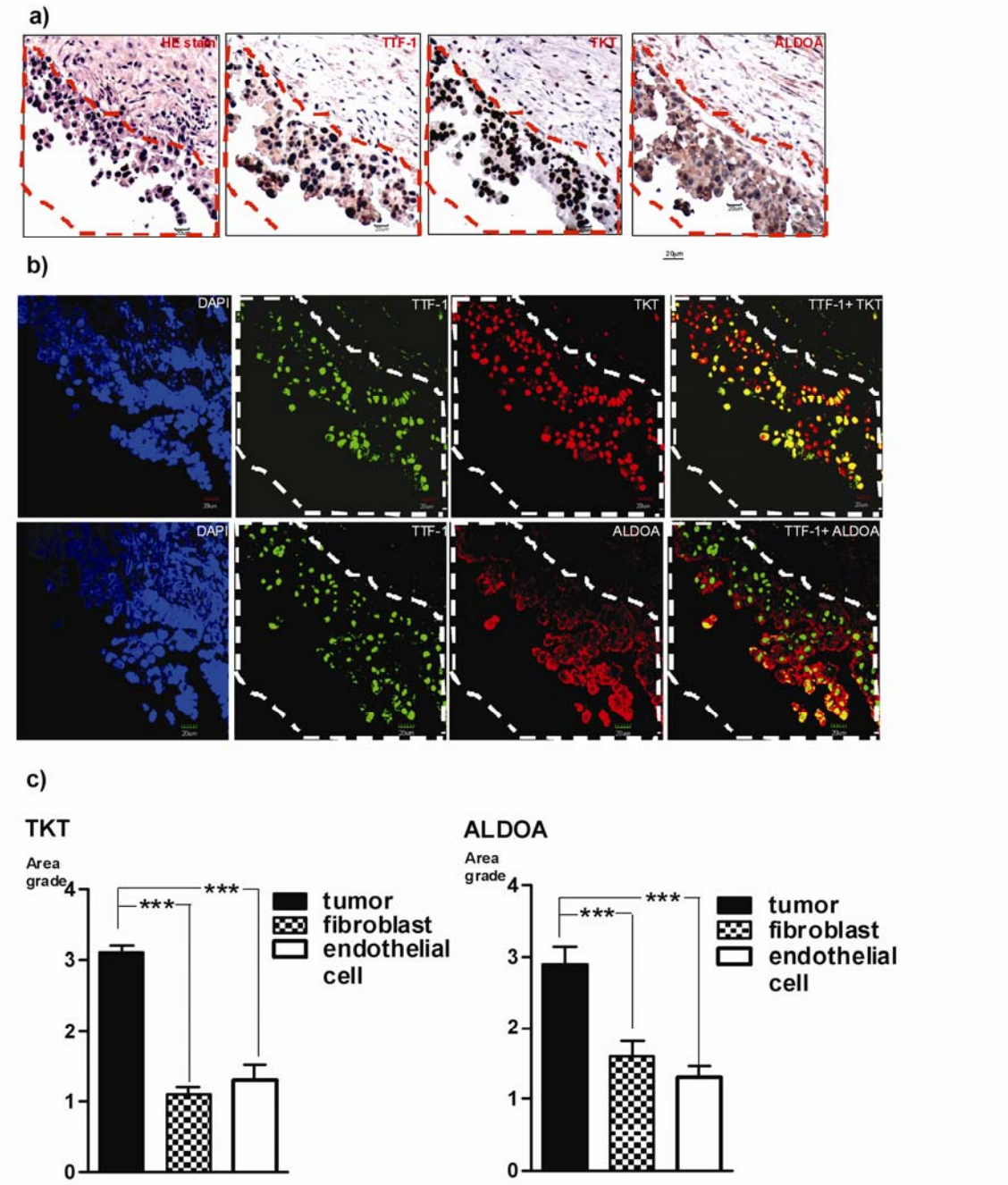

Figure 6. Inhibition of transketolase blocked the viability or proliferation of lung cancer cells. (a) Oxythiamine, a transketolase inhibitor, blocked the viability of lung cancer cells. The viability rate was detected using MTT test. (b) The knockdown of

TKT with TKT siRNA inhibited the proliferation of PC14PE6/AS2 cells. Western blotting analyses showed the expression of TKT of PC14PE6/AS2 cells transfected or untransfected with siRNA-scramble control, siRNA-TKT. (c) Histograms showed Ki-67 staining of TKT siRNA and scramble-transfected PC14PE6/AS2 cells compared to the isotype control. (d) Proportions of Ki-67 positive and colony formation in TKT siRNA or scramble-transfected PC14PE6/AS2 cells (**$p<0.01$).

FIGURE 6.

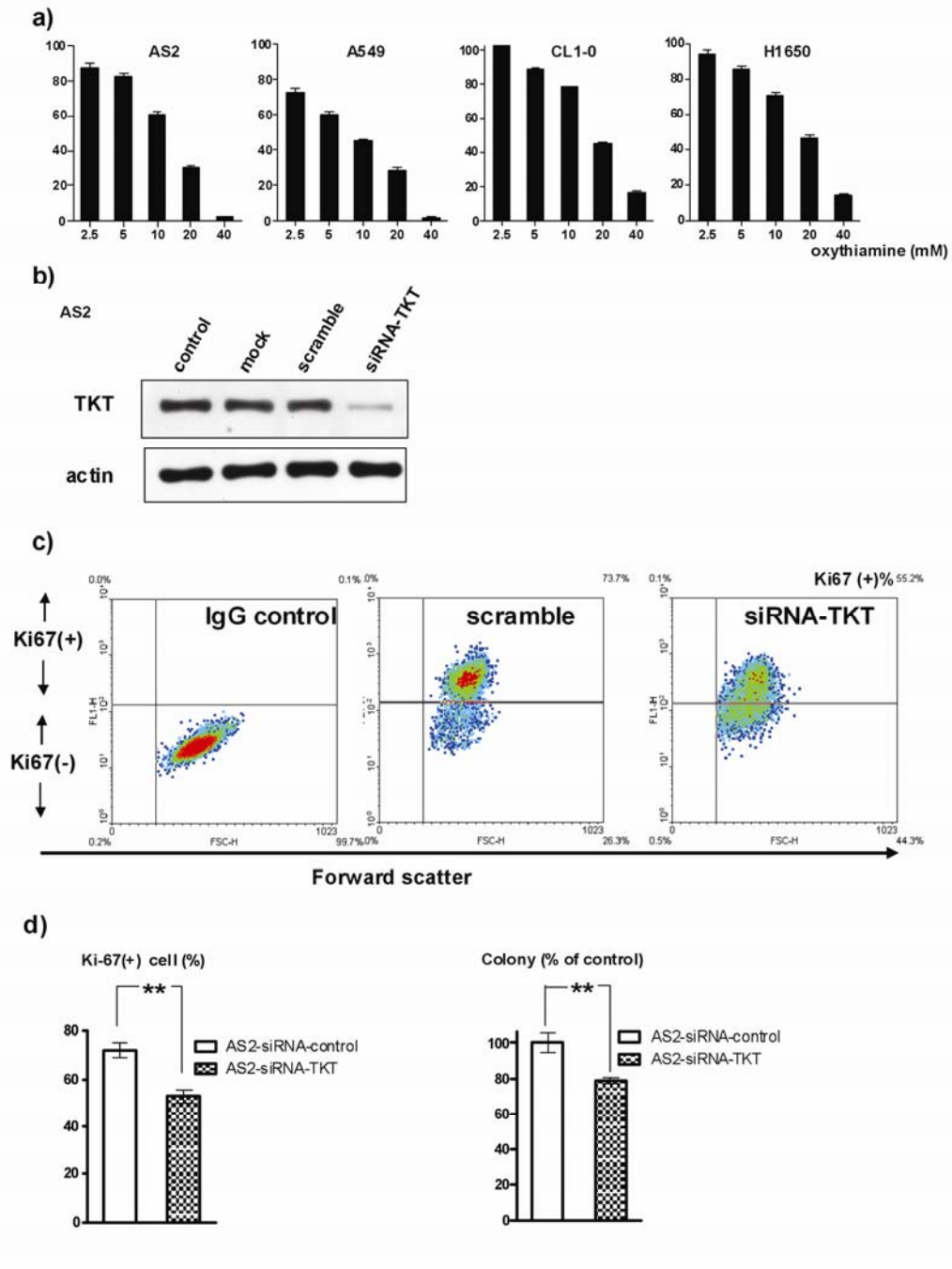

Figure 7. Inhibition of TKT in PC14PE6/AS2 cells reduced VEGF secretion and vascular permeability. (a) Secretion of VEGF of PC14PE6/AS2 was calculated after transfection with scramble siRNA or TKT siRNA and maintained in ultra-low

attachment plate (**p<0.01, n=4). (b) Biologic activity of VEGF secreted by PC14PE6/AS2 cells after transfection with scramble siRNA or TKT siRNA was measured by the Miles permeability assay. The dye leakage areas were marked by dashed red circles. (c) The areas of dye leakage were calculated for each injection site (*p<0.05, n=4).

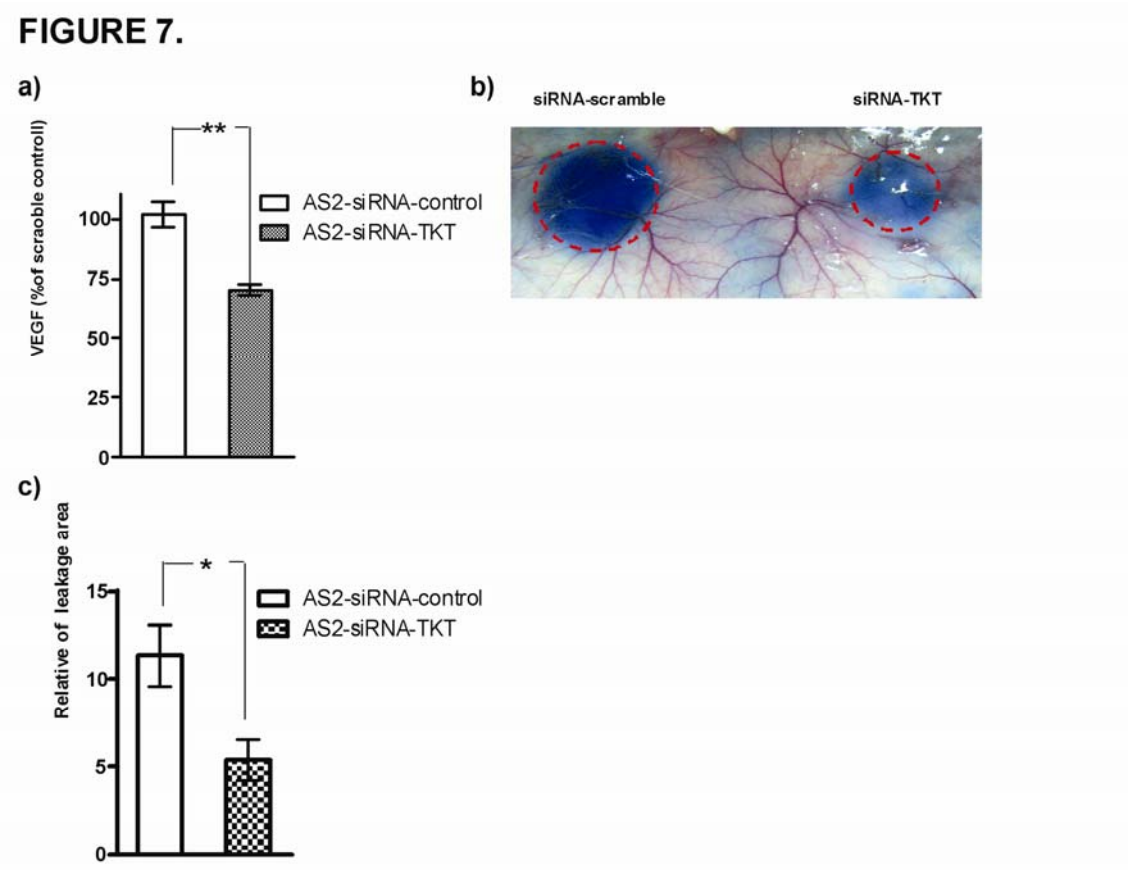

Supplementary

Figure 1. TKT and ALDOA (except CL1-0) were up-regulated and TSC1

down-regulated in lung cancer cell lines. Western blotting was used to detect TSC1, TKT, and ALDOA expressions in the lysates from normal bronchial cell line (NL-20) and lung cancer cell lines (PC14PE6/AS2, A549, CL1-0, H1650).

Figure 2. Immunohistochemistry analysis showed high expression of TKT and ALDOA in metastatic pleural tumor. (a) Nucleus immuno-reactive TKT were predominantly expressed in metastatic adenocarcinoma (20× objective), and the high magnitude (40× objective) of the red square area showed higher TKT intensity (oval area) in tumor than the adjacent fibroblasts (hollow arrow) and endothelial cells (arrow). (b) Cytoplasm immuno-reactive ALDOA were predominantly expressed in metastatic adenocarcinoma (20× objective), and the high magnitude (40× objective) of the red square area showed higher ALDOA intensity (oval area) in tumor than in adjacent fibroblasts (hollow arrow) and endothelial cells (arrow).